

# An oscillation-free finite volume method with staggered grids for solving problems of poroelasticity

\*Clovis R. Maliska<sup>1</sup> and Hermínio T. Honório<sup>1</sup>

<sup>1</sup>Department of Mechanical Engineering  
Federal University of Santa Catarina  
88040-900 – Florianópolis – SC - Brazil

\*Presenting and corresponding author: maliska@sinmec.ufsc.br

## Abstract

This paper advances a new finite volume alternative for solving poroelasticity problems employing a staggered arrangement for pressure and displacements in an unstructured grid framework. By staggering these variables, an improvement is obtained for the pressure-displacement coupling, which is claimed by the authors to prevent the numerical solution from instabilities in the pressure field. The two-dimensional formulation is still under development, but preliminary one-dimensional results are presented to demonstrate this capability. It is shown that the staggered formulation keeps second order accuracy for both pressure and displacement, even for highly non-uniform grids. In addition, the formulation does not present any spurious pressure oscillations, a key issue when solving poroelasticity problems under undrained conditions. The results suggest that staggering the rock displacements related to the pore pressure is a very promising approach to confer robustness to the numerical scheme. The novel method is founded on the analogy among pressure-velocity coupling for the Navier-Stokes equations and pressure-displacement for the poroelasticity problems. It is worth to mention that both physics are treated with the same conservative method.

Keywords: **Staggered grids, unstructured grids, numerical stability, poroelasticity**

## Introduction

Several engineering problems are modeled by systems of coupled partial differential equations, many of them involving different physics. In geomechanics, in which compacting porous media is coupled with the fluid flow, is one example. In this case, a delicate coupling between pore-pressure and rock displacement is present, since under certain conditions, as in the very beginning of the transient, or at the interface of two materials with different permeability, pressure wiggles appear in the numerical solution. Those situations, which resemble an undrained condition, impose an almost zero compressibility, which creates the condition for this pathology to appear. In the class of Finite Element methods, extensively used for solving the rock mechanics in porous media, several remedies for this pathology is available, being mixed finite element [1] and discontinuous Galerkin some of the possibilities. However, those remedies are at a cost of considerably increasing in computer time. Alternatively, some authors [2,3] have proposed stabilization techniques that do not increase the computational cost and still eliminate the instabilities, but at a cost of introducing numerical diffusion to the solution. Recently, in the context of finite volumes, Honório and Maliska [4] have proposed a strategy for avoiding such instabilities, which can be also regarded as a stabilization technique. In spite of all these alternatives, a numerical scheme that efficiently eliminates the pressure wiggles without increasing computational cost, while keeping the same order of accuracy for both pressure and displacements, is still pursued.

An analysis of the coupling between pressure and displacement for poroelasticity, and pressure and velocity for Navier-Stokes flows, reveals that they are of the same nature, so it is expected that the remedies employed in one class of problems can be applied to the other one with success. It should be recalled that the oscillatory pressure fields arising when solving incompressible Navier-Stokes flows, and its remedies, is known for more than four decades, and can be fully mitigated if a staggered grid approach is employed [5]. This remedy was abandoned when unstructured grids were required for solving fluid flows in complex geometries, due to the alleged complexity of implementation. This paper addresses this issue, advancing a finite volume method using unstructured grids with staggered variables, avoiding the oscillatory pressure field that appears in poroelasticity. Another important feature of the methodology herein presented is the solution of the both physics, fluid flow and rock mechanics, with the same finite volume technique [6].

Firstly, it is presented the mathematical model for the coupled poroelasticity problem. Then, the fundamentals of the staggered arrangement of variables are discussed, and a brief analogy is established between pressure-displacement in poroelasticity and pressure-velocity for Navier-Stokes flows. The model equations are discretized for two-dimensions and results are presented for 1D problem for both staggered and collocated arrangements. Finally, a few remarks close the work.

### Mathematical Model

The mechanical behavior of saturated porous media, besides being affected by its mechanical properties, it is also influenced by the pressure of the fluid filling its pores. Terzaghi [7] introduced the concept of effective stress into the equations of stress equilibrium in order to take the pore pressure into account, yielding

$$\nabla \cdot \boldsymbol{\sigma} - \alpha \nabla p = \mathbf{b} \quad (1)$$

in which  $\nabla$  is the nabla operator,  $\boldsymbol{\sigma}$  is the effective stress tensor,  $\alpha$  is the Biot coefficient,  $p$  is the pore pressure and  $\mathbf{b}$  is a source term. Moreover, considering small strains and a stress-strain relationship represented by the constitutive matrix  $\mathbf{E}$  (Voigt notation), the effective stress tensor can be written in terms of the displacement vector  $\mathbf{u}$  by the expression

$$\boldsymbol{\sigma} = \mathbf{E} \nabla_s \mathbf{u} \quad (2)$$

with  $\nabla_s$  being the symmetric nabla operator. The closure of the model is ensured by the mass conservation equation for deformed porous media, given by

$$\frac{1}{M} \frac{\partial p}{\partial t} + \nabla \cdot (\mathbf{v}^f + \mathbf{v}^s) = q \quad (3)$$

in which  $1/M$  is the Biot module and  $q$  is a source term. Equation (3) is conveniently written here in terms of the fluid velocity,  $\mathbf{v}^f$ , and the solid grains velocity,  $\mathbf{v}^s$ , which are respectively given by

$$\mathbf{v}^f = -\frac{\mathbf{k}}{\mu} \cdot \nabla p \quad (4)$$

$$\mathbf{v}^s = \frac{\partial \mathbf{u}}{\partial t} \quad (5)$$

with  $\mathbf{k}$  being the absolute permeability tensor and  $\mu$  the fluid viscosity. The gravitational term in equation (4) has been neglected with no loss of generality.

### *Staggered Grid Arrangement*

One of the major challenges faced by the numerical schemes developed to solve equations (1) and (3) is how to avoid pressure wiggles that can appear under undrained consolidation. In this situation the consolidation process takes place in a much smaller time scale than the fluid motion ( $\mathbf{v}^s \gg \mathbf{v}^f$ ), which yields the following mass conservation equation

$$\frac{1}{M} \frac{\partial p}{\partial t} + \nabla \cdot \mathbf{v}^s = q \quad (6)$$

Equation (6) is very similar to the mass conservation equation that appears when solving the Navier-Stokes equations. It is well known that satisfying this equation is of utmost importance to avoid the well-known checkerboard pressure problem [8]. The key issue in poroelasticity resides on how to determine a displacement field that satisfy both mass and momentum equations. For the Navier-Stokes equations the problem is exactly the same, except that the unknown variable is the velocity field instead of displacement.

Ensuring mass and momentum conservation is not a trivial task to be accomplished. The pioneering work to address this issue is due to Harlow and Welch [5], in the context of finite differences. They staggered the positions of pressure and velocities, such that momentum and mass conservation are satisfied for different control volumes but for the same set of variables. In this manner, pressure and velocities are directly available where they are required when integrating the corresponding partial differential equation in a control volume for mass or momentum. This technique is recognized to completely mitigate pressure wiggles for the Navier-Stokes equations. Due to the similarity of equation (6) with its counterpart in Navier-Stokes flows, a staggered grid arrangement between pressure and displacement might have strong chances to completely eliminate the pressure wiggles appearing in poroelasticity problems.

### **Finite Volume Formulation**

The traditional procedure for obtaining the approximate equations via a finite volume method starts by integrating the differential equations over each control volume. Since it is being proposed a staggered arrangement for  $\mathbf{u}$  and  $p$  the control volumes for pressure and displacement must be clearly identified. In this work, we follow the methodology presented by Peters and Maliska [9] for building the staggered control volumes on unstructured grids.

In figure (1a) it is shown the base mesh (the elements) provided by the grid generator. As depicted in figure (2b) the control volumes for mass conservation,  $\Omega^p$ , coincides with the elements of the base mesh. This control volume is for pressure. For the momentum equilibrium, however, the control volumes,  $\Omega^u$ , are built around the edges of the elements by connecting the vertices of the edge with the centroids of the two adjacent elements. A control volume  $\Omega^u$  is represented in figure (1c) and the position of  $\mathbf{u}_j$  is at the midpoint of the edge

of the element. The key point of this configuration is that the displacements are located at the faces of the control volume  $\Omega^p$  (figure (1b)), which will have a direct impact on the volumetric strain computation over  $\Omega^p$ , as will be shown later.

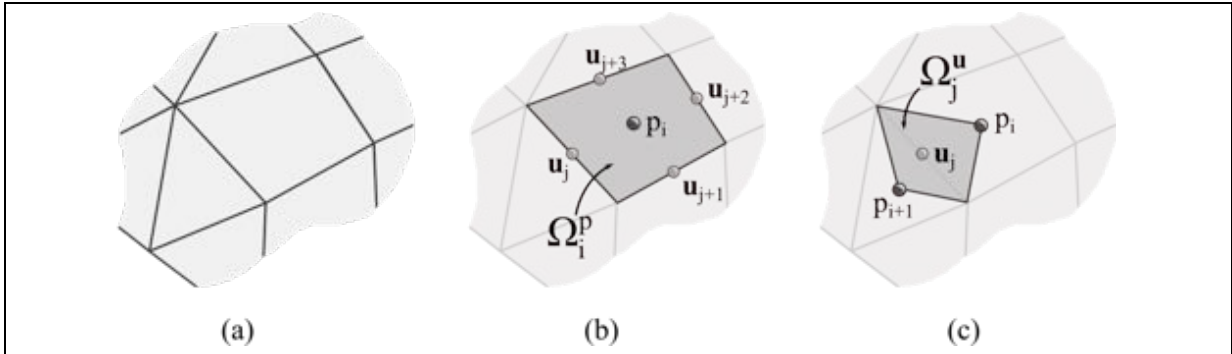


**Figure 1 Geometrical entities: (a) mesh composed by triangular and quadrilateral elements; (b) control volume for mass conservation and (c) control volume for momentum conservation.**

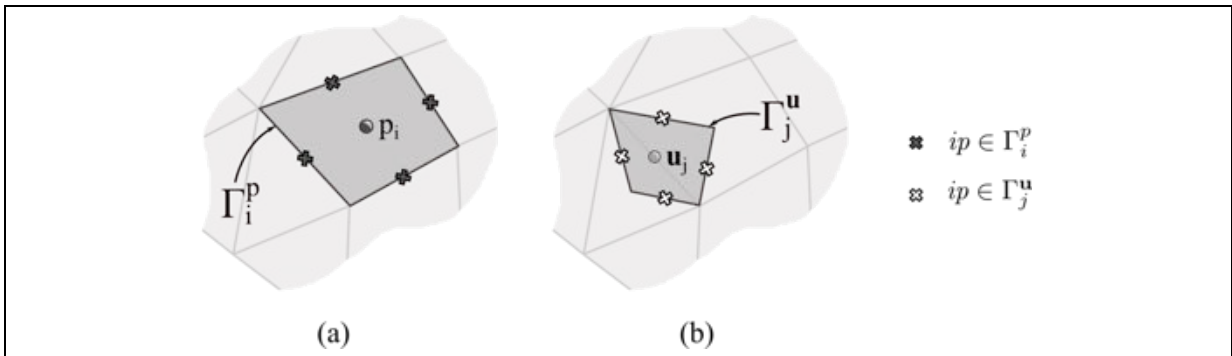


**Figure 2 Integration points (a) for mass and (b) for momentum**

### *Mass Conservation Equation*

Equation (3) is integrated over a time step,  $\Delta t$ , along with an implicit first-order backward Euler scheme and over the control volume  $\Omega_i^p$ . The divergence theorem is applied to obtain the surface integrals. By the midpoint rule, the semi-discretized form of equation (3) is

$$\frac{\Delta\Omega_i^p}{M} \frac{p_i}{\Delta t} + \sum_{ip \in \Gamma_i^p} \left[ (\mathbf{v}^f + \mathbf{v}^s) \cdot \mathbf{s} \right]_{ip} = q_i \Delta\Omega_i^p + \frac{\Delta\Omega_i^p}{M} \frac{p_i^o}{\Delta t} \quad (7)$$

in which the variables evaluated at the previous time level carries the superscript  $^o$ , and no superscript refers the current time level. Each control volume  $\Omega^p$  is bounded by a set of faces (or edges) and at the midpoint of each face is located an integration point  $ip$ . The set of integration points surrounding  $\Omega_i^p$  is denoted by  $\Gamma_i^p$ , as highlighted in figure (2). Each integration point has an area vector,  $\mathbf{s}_{ip}$ , pointing outwards the control volume. In addition, the volume of  $\Omega^p$  is represented by  $\Delta\Omega^p$ . Recalling equation (5), the mass fluxes crossing the faces of  $\Omega^p$  due to the rock deformation and fluid motion are, respectively, given by

$$w_{ip}^s \approx (\mathbf{v}^s \cdot \mathbf{s})_{ip} = \frac{(\mathbf{u}_{ip} - \mathbf{u}_{ip}^o)}{\Delta t} \cdot \mathbf{s}_{ip} \quad (8)$$

$$w_{ip}^p \approx (\mathbf{v}^f \cdot \mathbf{s})_{ip} = -\frac{1}{\mu} (\mathbf{k} \cdot \nabla p)_{ip} \cdot \mathbf{s}_{ip} \quad (9)$$

The main advantage of staggering  $\Omega^p$  and  $\Omega^u$  becomes clear by inspecting equation (8), noting that the displacement vectors  $\mathbf{u}_{ip}$  and  $\mathbf{u}_{ip}^o$  are directly available at the integration points of  $\Gamma_i^p$  (see figure (2)), avoiding any kind of interpolation. The benefits of this feature are of particular importance during undrained consolidation (equation (6)), where the mass fluxes through the control volume's faces is entirely given by  $w^s$ . This is precisely the point one is claiming to be the key point for avoiding the pressure instabilities.

The next step is to choose how to reconstruct the pressure gradient of equation (9) at the integration points belonging to  $\Gamma^p$ . The literature is abundant on these kind of methods, and Cerbato et al. [10] present an extensive analysis of several techniques for gradient reconstruction specifically applied to unstructured grids, which could be readily applied here to approximate equation (9). The reconstruction could also be done by a Multi-Point Flux Approximation (MPFA), as proposed by Aavastmark et al. [11].

### *Equilibrium Equations*

Equation (1) is integrated over the control volume  $\Omega_j^u$ , as depicted in figure (1c), and the divergence theorem is applied to the divergent operator yielding

$$\sum_{ip \in \Gamma_j^u} (\boldsymbol{\sigma} \cdot \bar{\mathbf{s}})_{ip} - \alpha \int_{\Omega_j^u} \nabla p \, d\Omega_j^u = \mathbf{b}_j \Delta \Omega_j^u \quad (10)$$

in which  $\Gamma_j^u$  is the set of integration points surrounding  $\Omega_j^u$ , as shown in figure (2b), and  $\bar{\mathbf{s}}$  is an appropriate arrangement of the area vector components, which for the two-dimensional case is

$$\bar{\mathbf{s}} = \begin{bmatrix} s_x & 0 \\ 0 & s_y \\ s_y & s_x \end{bmatrix} \quad (11)$$

The volumetric integral of the pressure gradient in equation (10) is approximated by the Green Gauss theorem

$$\int_{\Omega_j^u} \nabla p \, d\Omega_j^u \approx \nabla p_j \Delta \Omega_j^u \quad , \quad (12)$$

Now, it is important to notice that  $\nabla p_j$  is exactly the same as the pressure gradient required by equation (9), since a displacement position  $j$  always coincide with an integration point belonging to  $\Gamma_i^p$ , as it can be seen in figure (2). Therefore, the methodology chosen to evaluate equation (9) can be the same used to compute equation (12).

The remaining term to be evaluated in equation (10) is the stress tensor,  $\sigma_{ip}$ , at the integration point belonging to  $\Gamma_j^u$ . This is performed using equation (2). The procedure to compute the displacement derivatives  $\nabla_s \mathbf{u}$  at the integration points of  $\Gamma_j^u$  follows the approach presented in [9] for computing the velocity derivatives.

### One Dimensional Formulation

The corresponding 1D formulation of the methodology just described is now considered. The 1D formulation simplifies considerably the geometry, but still carries all the ingredients to evaluate the ability of the scheme to avoid pressure instabilities. Therefore, some preliminary results of the above formulation using the grid shown in figure (3) are presented. The results are compared with the traditional collocated arrangement of variables, as depicted in figure (4). It is worth to mention that the grids can be unequally spaced.

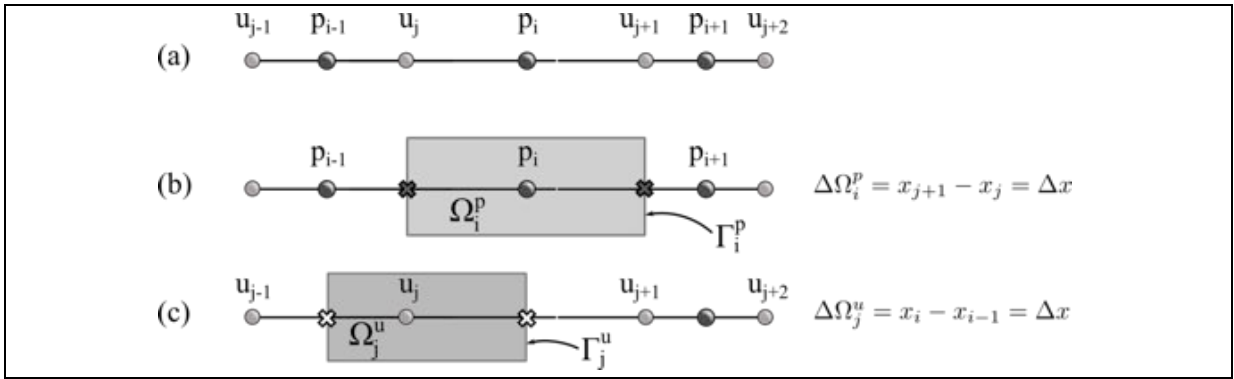


Figure 3 (a) 1D grid, (b) control volume for pressure and (c) control volume for displacement.

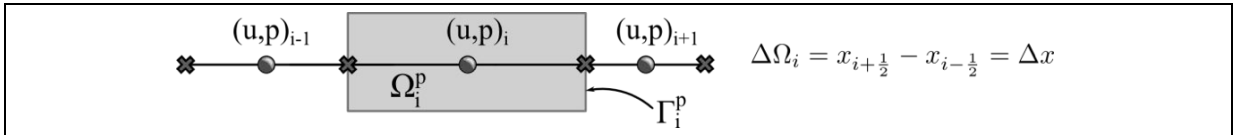


Figure 4: Collocated (coincident) control volumes associated to a 1D grid

#### 1D Staggered Grid Formulation

Integrating equations (3) and (1) over  $\Omega_i^p$  and  $\Omega_j^u$  of figure (3), respectively, results in

$$\frac{\Delta\Omega_i^p}{M} \frac{p_i}{\Delta t} - \frac{k}{\mu} \left( \left. \frac{\partial p}{\partial x} \right|_{j+1} - \left. \frac{\partial p}{\partial x} \right|_j \right) + \frac{\alpha}{\Delta t} (u_{j+1} - u_j) = \frac{\Delta\Omega_i^p}{M} \frac{p_i^o}{\Delta t} + \frac{\alpha}{\Delta t} (u_{j+1}^o - u_j^o) \quad (13)$$

$$\sigma_i - \sigma_{i-1} - \alpha(p_i - p_{i-1}) = 0 \quad (14)$$

with the following approximations at the integration points

$$\left. \frac{\partial p}{\partial x} \right|_{j+1} \approx \frac{p_{i+1} - p_i}{x_{i+1} - x_i} = \frac{p_{i+1} - p_i}{\Delta x_{j+1}} \quad (15)$$

$$\left. \frac{\partial p}{\partial x} \right|_j \approx \frac{p_i - p_{i-1}}{x_i - x_{i-1}} = \frac{p_i - p_{i-1}}{\Delta x_j} \quad (16)$$

$$\sigma_i = (\lambda + 2G) \left. \frac{\partial u}{\partial x} \right|_i \approx (\lambda + 2G) \frac{u_{j+1} - u_j}{x_{j+1} - x_j} = (\lambda + 2G) \frac{u_{j+1} - u_j}{\Delta x_i} \quad (17)$$

$$\sigma_{i-1} = (\lambda + 2G) \left. \frac{\partial u}{\partial x} \right|_{i-1} \approx (\lambda + 2G) \frac{u_j - u_{j-1}}{x_j - x_{j-1}} = (\lambda + 2G) \frac{u_j - u_{j-1}}{\Delta x_{i-1}} \quad (18)$$

The set of equations (13) and (14), along with equations (15-18), composes a linear system of equations for pressure and displacement that is solved in a simultaneous (monolithic) fashion.

### Co-located Formulation

The discretization of the equations for a collocated grid is basically the same as the previous case, except that the integration for both variables is performed over the same control volume  $\Omega_i$ . In this manner, the resulting equations are

$$\frac{\Delta \Omega_i}{M} \frac{p_i}{\Delta t} - \frac{k}{\mu} \left( \left. \frac{\partial p}{\partial x} \right|_{i+\frac{1}{2}} - \left. \frac{\partial p}{\partial x} \right|_{i-\frac{1}{2}} \right) + \frac{\alpha}{\Delta t} (u_{i+\frac{1}{2}} - u_{i-\frac{1}{2}}) = \frac{\Delta \Omega_i}{M} \frac{p_i^o}{\Delta t} + \frac{\alpha}{\Delta t} (u_{i+\frac{1}{2}}^o - u_{i-\frac{1}{2}}^o) \quad (19)$$

$$\sigma_{i+\frac{1}{2}} - \sigma_{i-\frac{1}{2}} - \alpha (p_{i+\frac{1}{2}} - p_{i-\frac{1}{2}}) = 0 \quad (20)$$

The approximations at the integration points still hold

$$\left. \frac{\partial p}{\partial x} \right|_{i+\frac{1}{2}} \approx \frac{p_{i+1} - p_i}{x_{i+1} - x_i} = \frac{p_{i+1} - p_i}{\Delta x_{i+\frac{1}{2}}} \quad (21)$$

$$\left. \frac{\partial p}{\partial x} \right|_{i-\frac{1}{2}} \approx \frac{p_i - p_{i-1}}{x_i - x_{i-1}} = \frac{p_i - p_{i-1}}{\Delta x_{i-\frac{1}{2}}} \quad (22)$$

$$\sigma_{i+\frac{1}{2}} \approx (\lambda + 2G) \frac{u_{i+1} - u_j}{x_{i+1} - x_i} = (\lambda + 2G) \frac{u_{i+1} - u_j}{\Delta x_{i+\frac{1}{2}}} \quad (23)$$

$$\sigma_{i-\frac{1}{2}} \approx (\lambda + 2G) \frac{u_i - u_{i-1}}{x_i - x_{i-1}} = (\lambda + 2G) \frac{u_i - u_{i-1}}{\Delta x_{i-\frac{1}{2}}} \quad (24)$$

It can be seen now that equations (19) and (20) require the evaluation of  $u$  and  $p$  at the integration points, where they are not available, due to the co-located arrangement. In this case, we use a linear interpolation of these variables, thus the following relationships are employed

$$p_{i+\frac{1}{2}} \approx \frac{\Delta x_{i+\frac{2}{3}} p_i + \Delta x_{i+\frac{1}{3}} p_{i+1}}{\Delta x_{i+\frac{1}{2}}} \quad (25)$$

$$p_{i-\frac{1}{2}} \approx \frac{\Delta x_{i-\frac{2}{3}} p_i + \Delta x_{i-\frac{1}{3}} p_{i-1}}{\Delta x_{i-\frac{1}{2}}} \quad (26)$$

$$u_{i+\frac{1}{2}} \approx \frac{\Delta x_{i+\frac{2}{3}} u_i + \Delta x_{i+\frac{1}{3}} u_{i+1}}{\Delta x_{i+\frac{1}{2}}} \quad (27)$$

$$u_{i-\frac{1}{2}} \approx \frac{\Delta x_{i-\frac{2}{3}} u_i + \Delta x_{i-\frac{1}{3}} u_{i-1}}{\Delta x_{i-\frac{1}{2}}} \quad (28)$$

in which  $\Delta x_{i+\frac{2}{3}} = x_{i+1} - x_{i+\frac{1}{2}}$ ,  $\Delta x_{i+\frac{1}{3}} = x_{i+\frac{1}{2}} - x_i$ ,  $\Delta x_{i-\frac{1}{3}} = x_i - x_{i-\frac{1}{2}}$  and  $\Delta x_{i-\frac{2}{3}} = x_{i-\frac{1}{2}} - x_{i-1}$ .

These two formulations will be used for solving the classical problem of poroelasticity, the Terzaghi's column, shown in Figure 5, with two main goals, to obtain the order of approximation of the staggered scheme, and demonstrate that the co-located grid arrangement without a stabilizing scheme is unable to dampen the pressure oscillations, while the staggered arrangement fully mitigate the pressure oscillations without any stabilizing scheme.

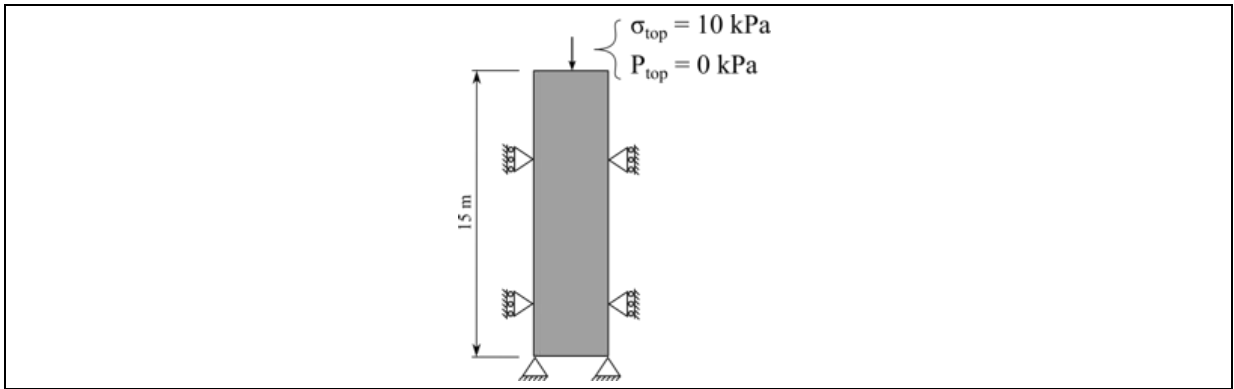


**Figure 5 Geometry and boundary conditions for the one-dimensional consolidation problem (Terzaghi's column).**

## Numerical Results

As depicted in figure (5), the domain has its bottom boundary fixed and impermeable, and the top boundary is fully-permeable ( $p_{top} = 0$  kPa) and subjected to a compressive load of  $\sigma_{top} = 10$  kPa. The structure is initially not deformed and the initial pore pressure equals to zero. The fluid phase properties are:  $\rho = 998,2$  kg/m<sup>3</sup>,  $\mu = 1,002 \times 10^{-3}$  Pa.s and  $c_f = 1,0 \times 10^{-4}$  MPa<sup>-1</sup>. The solid phase properties are:  $G = 1,732$  MPa,  $\lambda = 2,597$  MPa,  $\phi = 0,3$ ,  $\alpha = 1,0$  and  $K = 1,0 \times 10^{-4}$  m/s, where  $K$  represents the hydraulic conductivity.

The numerical solutions are now checked against analytical solutions for validation purposes, followed by an analysis of the order of approximation of the staggered scheme, concluding demonstrating that the staggered scheme is efficient in damping the pressure oscillations. Slightly and highly non-uniform spaced grids are employed. With a fixed time step size of 0,1 seconds, the pressure and vertical displacement profiles along the vertical direction are plotted against the analytical solution for specified time levels.

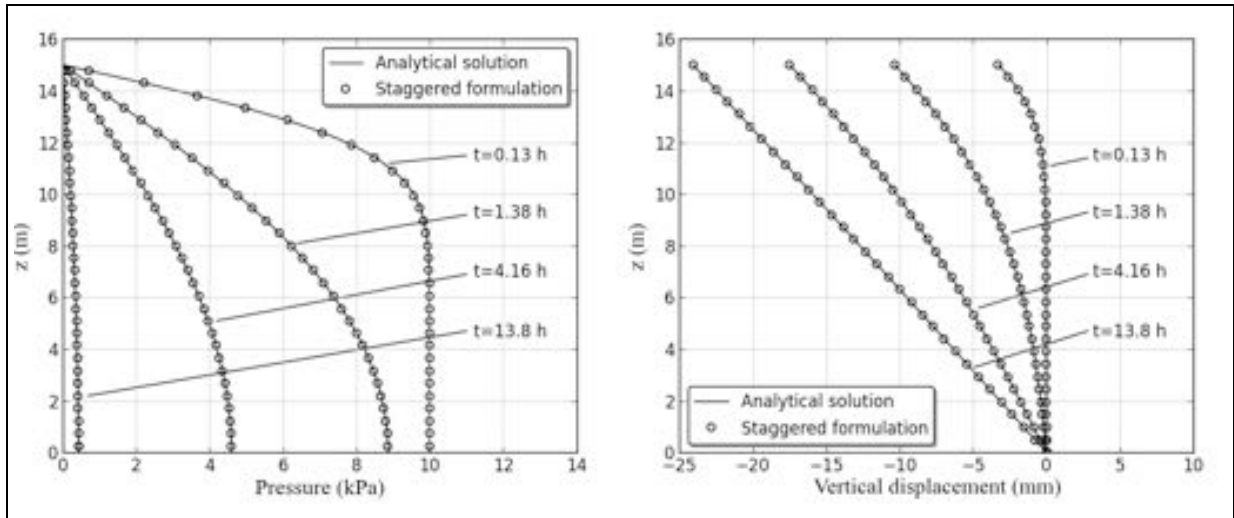


Figure 6 Pressure and displacement fields. Slightly non-uniform grid

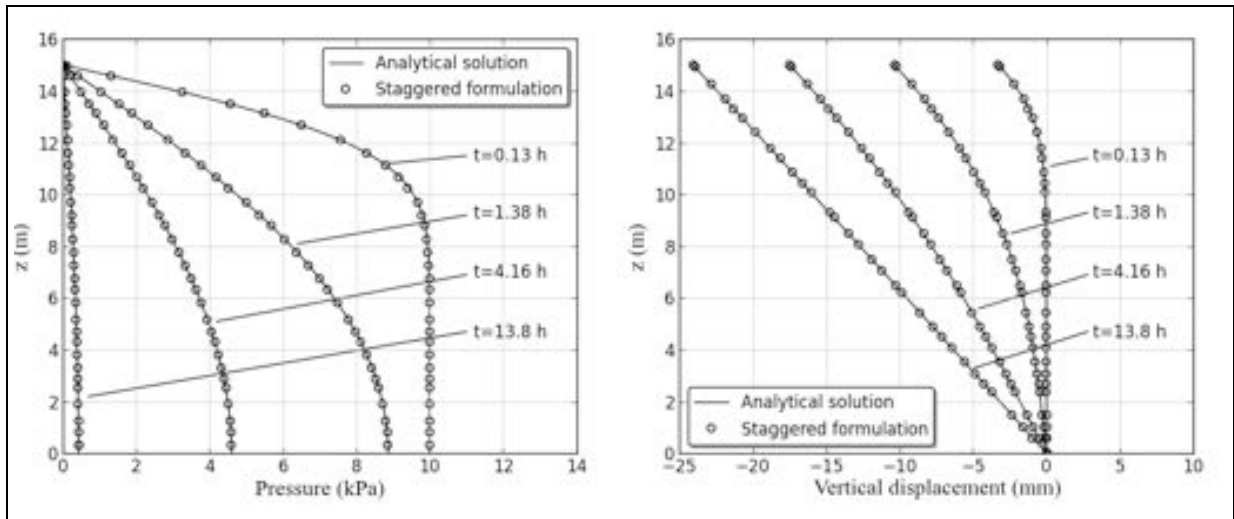


Figure 7 Pressure and displacement fields – Highly non-uniform grid

Figures (6) and (7) show the numerical and analytical solutions for the pressure and displacement profiles for slightly and highly non-uniform grids, indicating that the solutions are not affected by the non-uniformity of the grid.

### Convergence Analysis

The assessment of the convergence characteristics of the staggered scheme is performed considering two sets of progressively refined grids. The sets have slightly and highly non-uniform spaced grids randomly generated. For each set of grids, pressure and displacement profiles are taken at  $t = 500$  seconds. These profiles are compared with the analytical solutions and the Euclidean norm ( $L_2$ -norm) of the error vector is computed. Four different time step sizes are considered: 0,1, 1, 10 and 100 seconds.

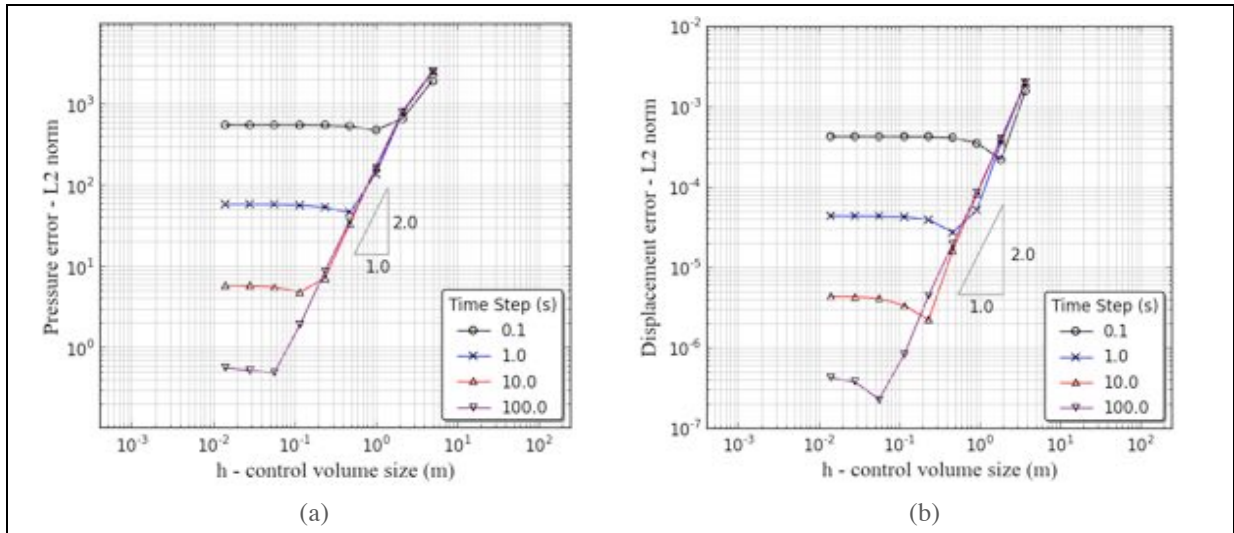


Figure 8 Convergence analysis of the staggered scheme for slightly non-uniform grid. (a) Pressure and (b) displacement.

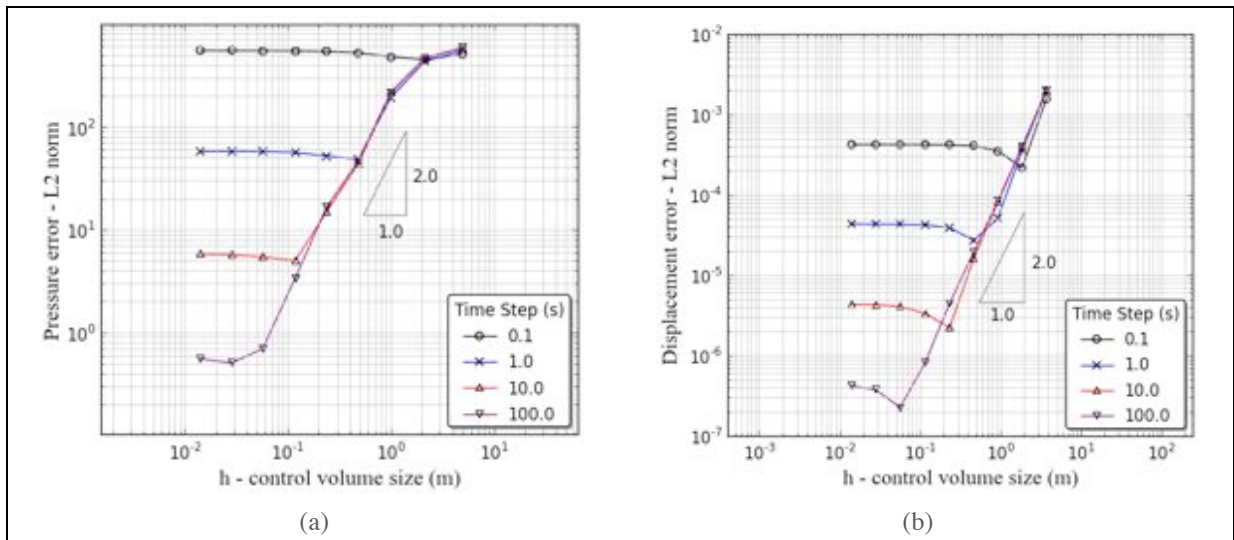


Figure 9 Convergence analysis of the staggered scheme for highly non-uniform grids. (a) Pressure and (b) displacement.

The behavior of the pressure and displacement error as the grid is refined is presented in figures (8) for slightly non-uniform grids. As can be seen, a second order decay of the error is obtained for both pressure and displacement. For highly non-uniform grid Figure (9b) shows second order of accuracy for displacement, while Figure (9a) suggests that the pressure is somehow affected by the grid non-uniformity, but it still can be regarded as a second order approximation.

#### Numerical Instabilities in the Pressure Field

As shown in the previous section, the staggered formulation is second-order accurate for pressure and displacement, even for highly non-uniform grids. It is well known that equal-order approximations for both pressure and displacement can cause numerical instabilities during undrained consolidation, where the fluid velocity is nearly zero. In this section, the same problem (Terzaghi's column) is solved with a time step size of 0,1 seconds and the

solution taken at  $t = 1,0$  second. In this situation the fluid does not have enough time to move as the solid matrix deforms, inducing an undrained consolidation. In fact, pressure instabilities are expected for equal-order formulations when the time step size is small enough to violate the minimum time step criteria postulated in [12]. This problem is solved with four different grids summarized as below

Grid 1	16 nodes	Slightly non-uniform
Grid 2	16 nodes	Highly non-uniform
Grid 3	32 nodes	Slightly non-uniform
Grid 4	32 nodes	Highly non-uniform

Table 1: Types of grids.

The numerical and analytical profiles are depicted in the figures below. The numerical solutions of the pressure and displacement profiles are obtained by both staggered and collocated arrangement of variables. Both numerical solutions are compared with the analytical one.

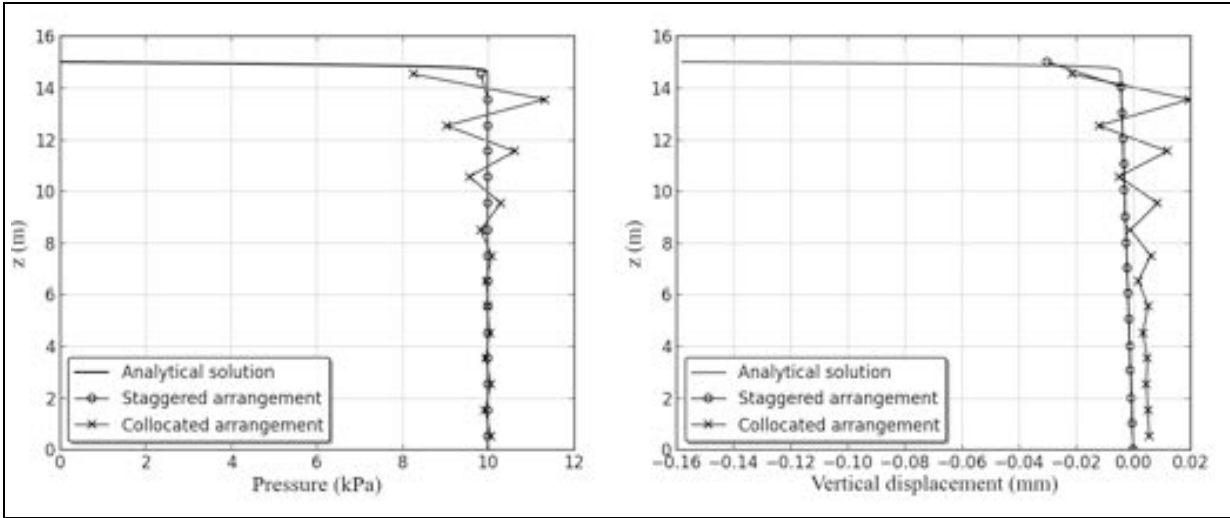


Figure 10 Pressure and displacement profiles for grid 1 (16 nodes).

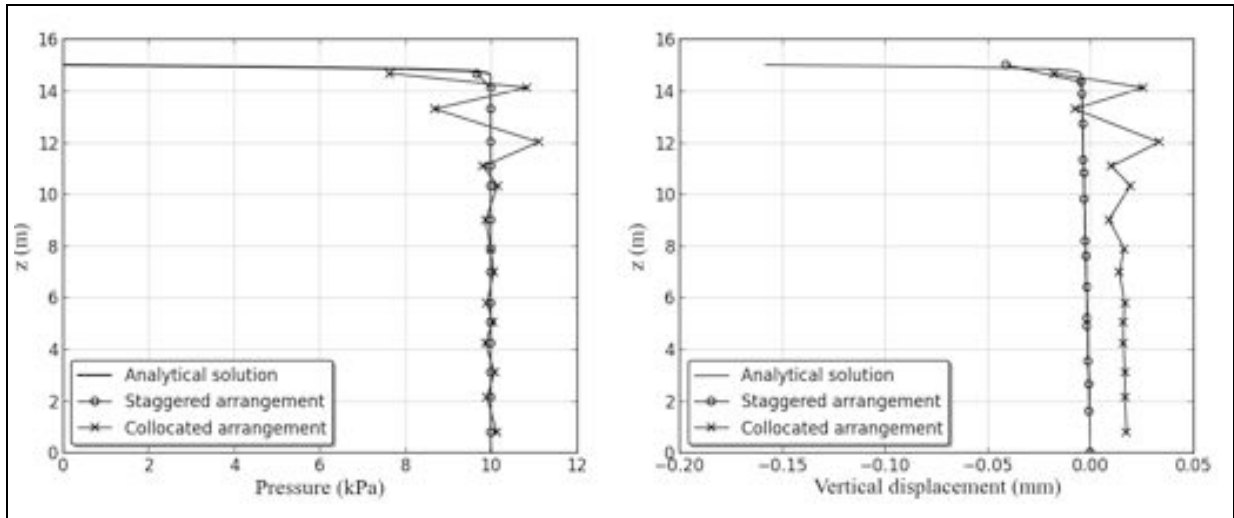


Figure 11 Pressure and displacement profiles for grid 2 (16 nodes).

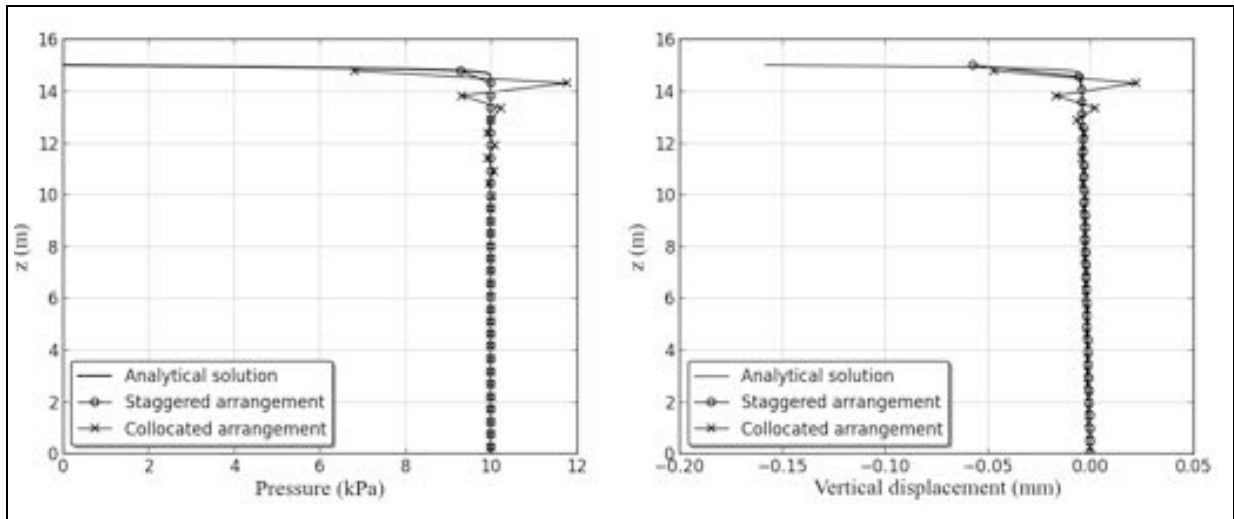


Figure 12 Pressure and displacement profiles for grid 3 (32 nodes).

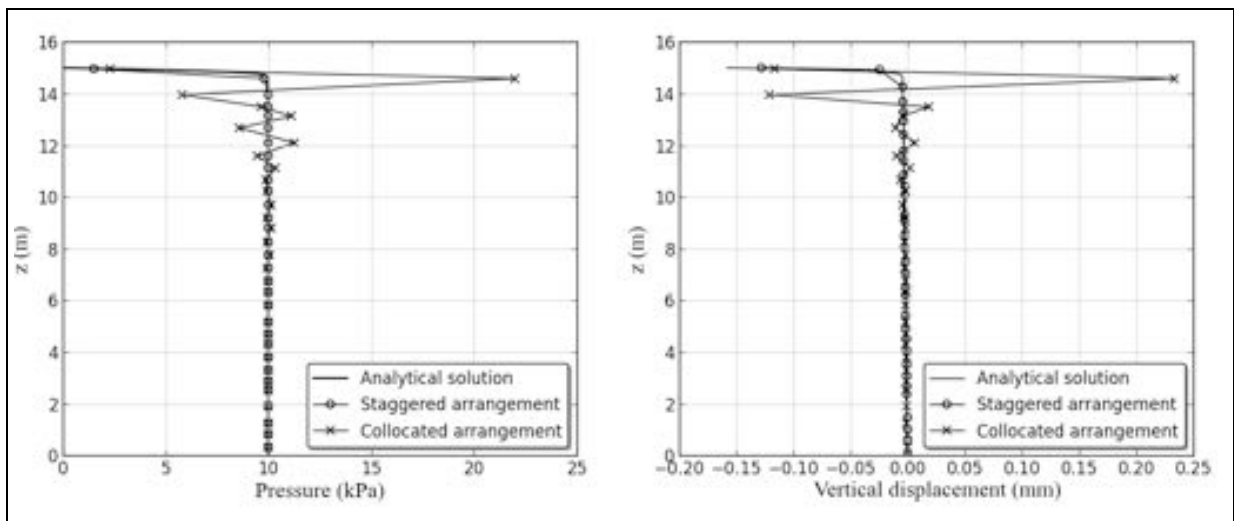


Figure 13 Pressure and displacement profiles for grid 4 (32 nodes).

As it can be seen in figures (10-13), the collocated formulation shows numerical instabilities also for the displacement field, what would be expected, since it directly depends on the

pressure gradient. For the grids with 16 nodes, figures (10) and (11) show an unacceptable solution obtained by the collocate formulation for the vertical displacement, which deteriorates even more with the grid non-uniformity. For the more refined grids (32 nodes), the numerical instabilities of the collocated arrangement concentrate along the upper-middle of the domain and they also get worse with the grid non-uniformity.

The staggered formulation, by its turn, despite presenting the same order of approximation for both pressure and displacement, does not show numerical instabilities at all. Instead, an excellent agreement is verified with the analytical solution. In addition, the staggered formulation for randomly spaced grids does not introduce any numerical diffusion, which is a common drawback of stabilization techniques commonly employed to equal-order formulations.

## Conclusions

In this work, a two-dimensional finite volume formulation has been presented for modeling the coupled fluid flow/geomechanics using staggered arrangement of variables for unstructured grids. An equivalent one-dimensional formulation for randomly spaced grids has been implemented and tested. The results show an overall second order accuracy for both pressure and displacement, even for highly non-uniform grids. Despite this fact, it has been shown that the staggered formulation does not present any numerical instability during critical situations and does not introduce any numerical diffusion to the solution. If this conclusion persists for 2D and 3D cases, and we believe it will since the 1D formulations carries the key reasons for the stability, the formulation advanced will generate poroelasticity solutions free from spurious oscillations, free from numerical diffusion and keeping second order of accuracy for both pressure and displacements, all embodied in a conservative scheme for mass, momentum and equilibrium equations.

## References

- [1] Ferronato, M., Castelletto, N. and Gambolati, G.: "A fully-coupled 3-D mixed finite element model of Biot consolidation", *Journal of Computational Physics*, vol. 229, pp. 4813-4830, 2010.
- [2] Choo, J. and Borja, R.I.: "A stabilized mixed finite elements for deformable porous media with double porosity", *Computer Methods in Applied Mechanics and Engineering*, vol. 293, pp. 131-154, 2015.
- [3] Preisig, M. and Prévost, J.H.: "Stabilization procedures in coupled poromechanics problems: A critical assessment", *International Journal for Numerical and Analytical Methods in Geomechanics*, vol. 35, pp. 1207-1225, 2011.
- [4] Honório, H.T. and Maliska, C.R.: "A stabilized finite volume method for solving one-dimensional poroelastic problems", *Rio Oil and Gas, Expo and Conference 2016 Proceedings*, Rio de Janeiro, 2016.
- [5] Harlow, F.H. and Welch, J.E.: "Numerical calculation of time-dependent viscous incompressible flow of fluid with free surface", *Physics of Fluids*, vol. 8, pp. 2182-2189, 1965.
- [6] dal Pizzol, A. and Maliska, C.R.: "A finite volume method for the solution of fluid flows coupled with the mechanical behavior of compacting porous media", *Porous Media and its Applications in Science, Engineering and Industry AIP Proc.*, 1453, pp. 205-210, 2012.
- [7] Terzaghi, K.: "Die berechnung der durchlässigkeitsziffer des tones aus dem verlauf der hydrodynamischen spannungsercheinungen", *Akademie der Wissenschaften, Wien Mathematisch-Naturwissenschaftliche Klasse*, 1923.
- [8] Patankar, S.V.: "Numerical Heat Transfer and Fluid Flow", Hemisphere Publishing Corporation, 1980.
- [9] Peters, R. and Maliska, C.R.: "A staggered grid arrangement for solving incompressible flows with hybrid unstructured meshes", *Numerical Heat Transfer, Part B Fundamentals*, vol. 71, pp. 50-65, 2017.
- [10] Cerbato, G., Hurtado, F.S.V., Silva, A.F.C. and Maliska, C.R.: "Analysis of gradient reconstruction methods on polygonal grids applied to petroleum reservoir simulation", *15th Brazilian Congress of Thermal Science and Engineering, ENCIT Proceedings*, Belém, 2014.

- [11] Aavastmark, I., Barkve, T., Bøe, O. and Mannseth, T.: " Discretization on unstructured grids for inhomogeneous, anisotropic media. Part I, Derivation of the methods", SIAM Journal on Scientific Computing, vol. 19, No. 5, pp. 1700-1716, 1998.
- [12] Vermeer, P.A. and Verruijt, A.: " An accuracy condition for consolidation by finite elements", International Journal of Numerical and Analytical Methods in Geomechanics, vol. 5, pp. 1-14, 1981.